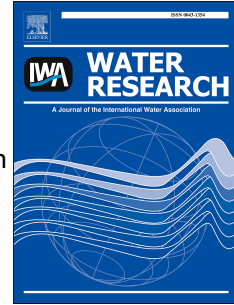


Accepted Manuscript

Impact of sludge layer geometry on the hydraulic performance of a waste stabilization pond

Faissal R. Ouedraogo, Jie Zhang, Pablo K. Cornejo, Qiong Zhang, James R. Mihelcic, Andres E. Tejada-Martinez



PII: S0043-1354(16)30329-3

DOI: [10.1016/j.watres.2016.05.011](https://doi.org/10.1016/j.watres.2016.05.011)

Reference: WR 12040

To appear in: *Water Research*

Received Date: 21 January 2016

Revised Date: 27 April 2016

Accepted Date: 2 May 2016

Please cite this article as: Ouedraogo, F.R., Zhang, J., Cornejo, P.K., Zhang, Q., Mihelcic, J.R., Tejada-Martinez, A.E., Impact of sludge layer geometry on the hydraulic performance of a waste stabilization pond, *Water Research* (2016), doi: 10.1016/j.watres.2016.05.011.

This is a PDF file of an unedited manuscript that has been accepted for publication. As a service to our customers we are providing this early version of the manuscript. The manuscript will undergo copyediting, typesetting, and review of the resulting proof before it is published in its final form. Please note that during the production process errors may be discovered which could affect the content, and all legal disclaimers that apply to the journal pertain.

1 **Impact of Sludge Layer Geometry on the Hydraulic Performance of** 2 **a Waste Stabilization Pond**

3 Faissal R. Ouedraogo* (fouedraogo@usf.edu), Jie Zhang, Pablo K. Cornejo, Qiong Zhang,
4 James R. Mihelcic, Andres E. Tejada-Martinez* (aetejada@usf.edu)

5 Department of Civil and Environmental Engineering, University of South Florida, 4202 E.
6 Fowler Ave., ENB 118, Tampa, FL 33620, USA

7 *Corresponding authors

8 **INTRODUCTION**

9 Wastewater stabilization ponds (WSPs) are a widely used and economically viable wastewater
10 treatment technology (Mara, 2004) that are critical for sanitation provision throughout the world.
11 Importantly this technology may be more sustainable than mechanized methods of wastewater
12 treatment (Muga & Mihelcic, 2008) and can be readily integrated with agricultural water reuse to
13 improve food security, especially for smaller cities facing increasing population and urbanization
14 (Verbyla et al, 2013a). In addition, such an approach can offset the negative impacts of
15 eutrophication while recovering valuable nutrients required for crop growth (Cornejo et al, 2013).
16 However, there are challenges in managing a WSP associated with parasite, bacteria, and virus
17 removal (e.g., Verbyla et al, 2013b; Verbyla & Mihelcic, 2015). The level of pathogen removal
18 is highly dependent on the hydraulic performance of a WSP (Verbyla & Mihelcic, 2015), which
19 also affects water quality parameters associated with suspended solids (SS) and biochemical
20 oxygen demand (BOD) (Lloyd et al, 2003; Nelson et al, 2004; Verbyla et al, 2013a). Therefore,
21 improving the hydraulic performance of a WSP is an important management strategy for not

22 only ensuring protection of public health and the environment, but also in maximizing the
23 potential to reuse the treated effluent.

24 Various mathematical models have attempted to analyze and optimize wastewater treatment
25 systems. Early studies on hydraulic performance of WSPs mainly employed reduced order
26 models, such as the completely mixed flow reactor (Ferrara & Harleman, 1981; Mayo, 1995),
27 ponds-in-series models (Canale et al, 1993), and dispersion models (Polprasert & Bhattarai,
28 1985). However these models are unable to capture flow structures, such as dead zones and
29 short-circuiting, resulting in less than optimal accuracy in predicting residence time distribution
30 and hydraulic performance. The rapid advance of computer technology has allowed
31 computational fluid dynamics (CFD) to be applied to wastewater treatment. CFD models have
32 been successfully applied for analysis and optimization of the hydraulics of WSPs in previous
33 studies (Wood et al, 1995; Wood et al, 1998; Peterson et al, 2000; Salter et al, 2000; Shilton,
34 2000; Vega et al, 2003; Karteris et al, 2005; Sweeney et al, 2005; Verbyla et al, 2013b).
35 Nonetheless, the predictions of CFD models on full-scale pond systems may be inaccurate due to
36 limited consideration of the physical conditions encountered in the field. For example, although
37 sludge accumulation is crucial to long-term maintenance of WSPs (Oakley et al, 2012), only a
38 few studies have incorporated sludge accumulation into CFD analysis (Murphy, 2012; Alvarado
39 et al, 2012). Murphy (2012) and Alvarado et al (2012) found that sludge distribution or geometry
40 influences hydraulic performance. For example, the hydraulic performance in a wastewater
41 stabilization pond when sludge is mostly deposited near the edges (e.g. Murphy, 2012) differs
42 from the hydraulic performance when an equal volume of sludge accumulates mainly near the
43 inlet or inflow (e.g. Alvarado et al, 2012). Murphy (2012) also demonstrated that sludge surface

44 roughness affects hydraulic efficiency of a pond by changing dispersion. Alvarado et al (2012)
45 found that sludge accumulation patterns and velocity profiles are interrelated and directly affect
46 pond hydraulic performance. However, in depth quantification of how advective transport and
47 associated flow patterns are affected by sludge accumulation and alter the WSP hydraulic
48 performance is needed.

49 In a WSP integrated with downstream beneficial reuse of water and embedded nutrients, the
50 pond effluent is allowed to enter an irrigation system. Changes in the operation of the system
51 may cause a water surface level increase in the pond, which can also affect the hydraulic
52 performance (Mercado et al, 2013). An increase in water surface level may also occur due to an
53 increase in sludge volume if the equal flow rates entering and exiting the pond are kept constant.
54 Accordingly, the objective of this study is to investigate the impact of different sludge volume
55 and accumulation patterns in conjunction with changes in water surface elevation on the
56 hydraulic performance of a WSP. Normally, in a WSP, changes in water surface elevation are
57 accompanied by changes in flow rate. However, in the present study, CFD simulations with
58 various water surface elevations were performed with a fixed flow rate in order to isolate
59 (highlight) the effect of the former on hydraulic performance.

60 A community managed wastewater stabilization pond in rural Bolivia was selected for this study,
61 which is representative of a WSP utilized in a developing country. Flow and tracer transport
62 simulations were conducted for this pond using a numerical solver of the three-dimensional
63 Reynolds-averaged Navier-Stokes equations (RANS). Sludge geometry as well as pond
64 geometry and water flow parameters obtained in the field are used to model the pond. The RANS
65 solver is then used to predict the hydraulic performance of the WSP under future sludge

66 accumulation scenarios. Numerical tracer studies on the pond with measured and potential future
67 sludge layer geometries are conducted to analyze the impact of sludge geometry on the hydraulic
68 performance of the WSP and to establish the importance of short and long term monitoring of
69 WSPs. Numerical tracer studies are also conducted with two different water surface elevations to
70 determine the impact of the surface level change on hydraulic performance of the pond.

71 The CFD analysis of the WSP in Bolivia offers a case study of the effects of sludge
72 accumulation and water surface level change on pond hydraulic performance. This is important
73 because WSPs are non-ideal reactors; thus, the creation of short circuits and dead zones can have
74 a large influence on pathogen removal (Verbyla & Mihelcic, 2015), which is critical for
75 performance, whether the pond is managed only for treatment or is integrated with a strategy of
76 resource recovery and reuse. Furthermore, WSP operators generally argue that sludge
77 accumulation is damaging because it reduces available pond volume and thus treatment capacity,
78 as well as hydraulic efficiency. Reduction in hydraulic efficiency would be expected given that a
79 reduction in available pond volume can lead to a reduction of the theoretical residence time
80 calculated as $\tau = \text{volume}/\text{flow rate}$. The validity of this argument will be examined via the CFD
81 analysis presented here. In the process, the current analysis highlights CFD as a potential tool
82 that could be used to establish a desludging schedule helping to minimize desludging cost while
83 maintaining adequate treatment capacity levels. Furthermore, the CFD model allows WSP
84 operators to determine a water surface level range that will not have significant consequences on
85 the effluent quality. At the design stage, application of CFD to a WSP should allow designers to
86 account for sludge accumulation and water level changes so a more sustainable and better

87 performing WSP can be integrated with resource recovery strategies that reuse valuable water
88 and nutrients.

89 **METHODOLOGY**

90 The wastewater stabilization pond system of focus here was designed to serve a population of
91 420 people in 2006 and served 780 people in 2012. The system consists of a facultative pond
92 followed by two maturation ponds, and is representative of a community managed WSP system
93 commonly found in the developing world (Cornejo et al, 2013). There are no baffles designed
94 into this system to direct pond influent or effluent. Details on sludge accumulation, water quality
95 (e.g., pathogen, nutrient, TSS, and BOD removal), life cycle cost, and life cycle impacts (e.g.,
96 carbon footprint, embodied energy, and eutrophication potential) can be found in previous
97 studies (Fuchs & Mihelcic, 2011; Verbyla et al, 2013a; Cornejo et al, 2013; Symonds et al, 2014).
98 Lizima (2012) and Verbyla et al. (2013a,b) have performed a study of this system that included
99 the measurement of sludge accumulation at the bottom of the pond; this information on sludge
100 accumulation is incorporated in the model development of the present study. The CFD
101 methodology employed here is based on the RANS equations and is a common and proven
102 accurate approach for modeling flow in water and wastewater treatment (Alvarado et al, 2012;
103 Zhang et al, 2013a, b; Zhang et al, 2013; Zhang et al, 2014a,b). In this approach, the mean flow
104 is computed explicitly and the unresolved turbulence is modeled or parameterized. The RANS
105 turbulence model used in the present study is the well-known $k-\varepsilon$ (*k-epsilon*) model equipped
106 with standard wall functions (Wilcox, 2004). In order to analyze characteristic residence times, a
107 passive tracer study was performed using the RANS flow solution. The turbulent Schmidt

108 number denoting the ratio of turbulent viscosity of the flow to turbulent diffusivity of the tracer
109 was set to 0.7, similar to other studies (Lauder, 1978; Zhang et al, 2014a).

110 Figure 1A provides the dimensions of the WSP modeled. A fixed flow rate boundary condition
111 was used for the inflow at the inlet of the pond (see Figure 1A). That is, the volumetric flow rate
112 at the inlet was fixed as 66 m³/day, which is an average flow rate measured in the field by Lizima
113 (2012) and Verbyla et al. (2013a,b). This flow rate corresponds to a theoretical residence time of
114 27.6 days (volume of pond/flow rate). Once the steady state RANS solution of the flow was
115 computed, the scalar advection-diffusion transport equation for the passive tracer was solved
116 using the flow velocity. The numerical tracer study was conducted by initially releasing a tracer
117 with concentration $C = 1$ (g/L) at the inlet over a 1020-second or 17-min period which is about
118 0.04% of the theoretical residence time. At the outlet of the pond, at the sidewalls and the bottom,
119 the normal gradients of C were set to zero indicating zero diffusive flux across these boundaries.

120 In analyzing results from the tracer transport simulation, the theoretical residence time, the mean
121 residence time (MRT), the short-circuiting index S (Persson, 2000), the moment index (Wahl et
122 al, 2010), and the relative moment index (Murphy, 2012) were used. Please refer to Teixeira &
123 Siqueira, 2008 for further details. The short-circuiting index is defined as

$$S = \frac{t_{16}}{\tau} \quad (1)$$

124 where τ is the theoretical residence time and t_{16} denotes the time it takes for 16 percent of the
125 tracer injected at the inlet to exit the pond. The intensity of short-circuiting decreases with
126 increasing value of S . A value of S equal to 1.0 corresponds to an ideal plug flow reactor (PFR)

127 and thus no short-circuiting occurring within the pond. Moment analysis of the normalized
 128 residence time distribution (RTD) is a tried and tested technique used to describe the distribution
 129 (Kadlec & Knight, 1996; Werner & Kadlec, 1996; Holland et al, 2004; Min & Wise, 2009; cited
 130 in Wahl et al, 2010). Unlike the short circuiting index, the moment index is not greatly
 131 dependent on the parcel of tracer exiting the pond fastest. Rather, it is more representative of the
 132 overall shape of the RTD curve without being heavily affected by the RTD long tail, which can
 133 lead to over-prediction of the residence time (Wahl et al, 2010). The moment index is defined as

$$134 \quad \text{Moment index} = 1 - \int_0^1 (1 - \theta) F(\theta) d\theta \quad (2)$$

135 where $F(\theta)$ is the cumulative residence time distribution function.

$$136 \quad F(\theta) = \int_{t=0}^{t=\tau} \frac{C_t}{C_{nominal}} \frac{1}{\tau} dt \quad (3)$$

137 where C_t is the tracer concentration at time t and $C_{nominal}$ is the nominal tracer concentration
 138 defined as

$$139 \quad C_{nominal} = \frac{\text{tracer concentration} \times \text{tracer release time}}{\text{theoretical residence time}} \quad (4)$$

140 The relative moment index is derived from the moment index while incorporating the decrease in
 141 water volume capacity as a result of sludge accumulation:

$$\text{Relative Moment index} = \text{Moment index} \times \frac{\text{Volume of water}}{\text{Initial volume of water}} \quad (5)$$

142 The moment index and the relative moment index are directly proportional to the pond hydraulic
143 efficiency while the relative moment index also takes into account the reduction in pond volume
144 and thus reduction in treatment capacity.

145 In order to project sludge accumulation in the pond, an empirical method (Oakley, 2005) was
146 utilized. This method predicts the annual volume of sludge (V_L in m^3 /year) as

$$V_L = 0.00156 \times Q_{av} \times SS \quad (6)$$

147 where Q_{av} is the average flow rate in m^3 /day and SS is suspended solids in the influent in mg/L.
148 In the present study, the value of SS measured in 2012 was 242 mg/L (Verbyla et al, 2013a) and
149 was assumed to have remained constant from 2006 through 2016. The annual average flow rate
150 Q_{av} was computed taking into account future growth in population according to the Malthus
151 exponential model (Brauer & Castillo-Chávez, 2011). Based on the previously described
152 methods, the prediction for the sludge volume accumulated between 2006 (when the pond had
153 no sludge) and 2012 given by equation eqn. (6) was $164 m^3$, which is approximately 6.5% higher
154 than the physically measured data (Lizima, 2012). Thus this method is seen to lead to good
155 predictions of future sludge accumulations.

156 Note that following the Mathus exponential model, the average annual flow rate increases in
157 proportion to population over the years as was considered for the calculation of accumulated
158 sludge volume V_L , previously described. However, for all CFD simulations performed the flow
159 rate was taken to be constant ($66 m^3/day$) in order to isolate sludge and water surface elevation
160 effects on hydraulic performance.

161 Four simulation cases, described in Table 1, were developed to analyze sludge geometry effects.
162 Case I corresponds to the WSP in 2006 when it was newly built and thus had no sludge. Case II
163 corresponds to the WSP in 2012 with sludge volume and distribution measured by Lizima (2012).
164 Using the sludge volume equation of Oakley (2005) (i.e. equation (6)) along with the Malthus
165 population growth model as described earlier, the sludge volume for 2016 was estimated as 326
166 m³. Two different sludge layer geometries or distributions for the 2016 sludge volume (to be
167 denoted as Cases III and IV) were considered following two assumptions: 1) the first assumption
168 is that the increment of sludge volume from 2012 to 2016 will mostly accumulate on top of the
169 existing sludge. The height of sludge in this scenario is assumed to increase uniformly by the
170 same percentage everywhere (Case III); 2) the second assumption is that the incoming sludge
171 deposits primarily in the flat area of the pond (Case IV). In this scenario, the peak sludge
172 elevation is the same as in Case II and not as high as in Case III (see Figure 2). The assumed
173 sludge accumulation geometries represent two extreme situations, where the actual sludge layer
174 geometry should be an intermediate between these two distribution conditions. Finally note that
175 the water surface elevation for the previously described cases (I-IV) was kept constant (see Table
176 1).

177 In order to investigate effects of changes in water surface level, two approaches at setting the
178 surface level for 2016 scenarios are followed. The sludge and water volumes measured in the
179 field in 2012 by Lizima are used as reference to set the water volume and associated water
180 surface levels. The water volume in 2012 was taken to be the total pond volume minus the sludge
181 volume measured in the field. In one approach the water surface level for 2016 scenarios was set
182 equal to the surface level measured in 2012 (1.8 m from the lowest point of the bottom of the

183 pond), corresponding to Cases III and IV in Table 1. In the second approach the water surface
184 level for 2016 scenarios was selected to preserve the 2012 measured water volume; this
185 corresponds to cases IIIA and IVA in Table 1. This table shows the water volumes, sludge
186 volumes and corresponding water surface levels for all cases. Note that Cases III and IIIA have
187 the same sludge volume and distribution and the only difference in these simulation cases is in
188 the water surface level. The same can be stated for Cases IV and IVA.

189

190 **MESH AND NUMERICAL TOOL**

191 As measured by Lizima (2012) the dimensions of the computational WSP are taken as $46 \text{ m} \times$
192 $23.9 \text{ m} \times 1.8 \text{ m}$ (length \times width \times depth). The computational domain based on these dimensions
193 along with the bottom sludge layer also measured by Lizima (2012) in 2012 is shown in Figure 1
194 (panels A, B and C). Based on grid independence studies (described further below), the total
195 number of tetrahedral cells for the computational model of the previously described pond
196 geometry was taken to be approximately 0.8 million and is shown in Fig. 1C. This computational
197 grid was refined near the walls, sludge and inlet/outlet so as to adequately resolve sharp gradients
198 in velocity expected in these regions. Similar grids were used to simulate the various scenarios
199 with different sludge geometries and water elevations described earlier. The RANS solver
200 employed well-known finite volume discretization techniques in OpenFOAM (2011).

201 **RESULTS AND DISCUSSION**

202 **Grid Refinement Study**

203 A grid refinement study is a common technique in the CFD domain for determining
204 the dependence of results on grid size and thus on discretization (numerical) error. The present

205 grid refinement study was comprised of four grids for the WSP for Case II from relatively fine to
206 coarse grids: 0.8 million elements, 0.4 million elements, 0.1 million elements and 0.05 million
207 elements. Figure 3 shows RTD of the passive tracer obtained on all 4 grids. Minor differences
208 can be seen between results on the 0.4 and 0.8 million element grids, indicating that the 0.8
209 million element mesh is sufficient for nearly grid independent results.

210

211 Note that RTD data measured in the field by Lizima (2012) has been deemed under-sampled for
212 comparison with the current computations, and thus such a comparison is not presented.
213 However, note that the CFD model used here has been validated in terms of RTD for other flow
214 configurations (or geometries) for which fully resolved experimental RTD data is available such
215 as flows in baffled and column contactors (Zhang et al. (2013a) and Zhang et al. (2014a,b)).
216 These validation studies have shown that the present numerical model is able to predict RTDs in
217 excellent agreement with laboratory and field measured data. In some of these cases the complex
218 flow geometry has produced richer flow structures than in the WSP of the current study, leading
219 to the conclusion that results for the present WSP are robust.

220

221 **Impact of sludge layer geometry on hydraulic performance**

222 Next, results from flow and tracer transport simulations are presented for Cases I-IV described
223 earlier through Table 1 and Figure 2.

224 Figure 4 shows water flow speed contours on x - y (horizontal) planes at the water surface (A, B,
225 C, D) and at depth of 0.69 m (E, F, G, H) from the water surface for Cases I-IV. Note that the
226 0.69 m depth corresponds to the depth of the inlet and outlet of the pond for the four cases. At

227 0.69 m depth (Figures 4E-H), a high-speed jet can be observed originating from the inlet in all
228 four scenarios, as expected. However, the sludge accumulation in Cases II, III and IV obstructs
229 the path of the jet forcing it to flow laterally around the sludge and vertically over the sludge.
230 The lateral re-direction of the jet caused by the sludge can be considered analogous to the lateral
231 re-direction of the flow caused by baffles in a baffled reactor. As will be quantified further below
232 via numerical tracer studies, this baffling effect caused by the sludge for certain sludge
233 accumulation patterns, such as that in Case III, can enhance the hydraulic efficiency of the pond
234 relative to the no-sludge scenario (Case I).

235 In Case III, the jet emanating from the inlet is primarily forced to change direction laterally
236 around the sludge whereas the jet in Cases II and IV is primarily forced to change direction
237 vertically over the sludge. The reason for this is that the sludge peak (or maximum height) in
238 Case III reaches closer to the water surface than in the other cases extending over 90% of the
239 total depth of the pond. This difference between the jet paths caused by the various sludge
240 scenarios can be seen at depth = 0.69 m by comparing Figures 4F, 4G and 4H. Here it can be
241 seen that flow speeds are greater around the sludge in Case III, indicative of the jet bending
242 around this obstacle. In Cases II and IV, rather than bending around the sludge, the jet travels
243 over the sludge and out of view from the plane at 0.69 m depth shown in Figs. 4F and 4H. After
244 the jet goes over the sludge it goes back down and into view of the 0.69 m depth plane as also
245 seen in Figs. 4F and 4H. As a result, in Cases II and IV, the flow is not seen to be as intensified
246 around the sludge at this depth compared to Case III. It may be concluded that the baffling effect
247 induced by the sludge is greater in Case III compared to Cases II and IV. A greater baffling

248 effect in Case III is expected to give rise to greater hydraulic efficiency, as will be shown further
249 below in terms of tracer studies and associated residence time characteristics.

250 Although the jets in Cases II-IV are obstructed by the sludge, they still travel for a certain
251 distance at a relatively high speed compared to the jet in Case I for which no sludge layer is
252 present. Similar high-speed jet flows can be observed in all four cases at the water surface
253 (Figures 4A-D). The high-speed jet flow in all cases establishes a highway from inlet to outlet
254 resulting in what is often referred to as short-circuiting. This so-called highway or short-circuit
255 may be observed in terms of flow streamlines in Figure 5. The high-speed jet can transport
256 particles, such as dye tracer, suspended solids and pathogens, much faster than the flow in other
257 parts of the pond, serving as a detriment to the hydraulic efficiency of the pond.

258 Comparing Figures 4A and B, it can be observed that the surface jet flow in Case II (Figure 4B)
259 is more intense than that in Case I (Figure 4A). The accumulated sludge in Case II effectively
260 reduces the cross-sectional area through which the near-surface flow travels, ultimately
261 enhancing the surface jet relative to the no-sludge scenario (Case I) consistent with Bernoulli's
262 principle and conservation of mass.

263 Figures 4B, 4D, 4F and 4H demonstrate that the jet path in Case IV is similar to that in Case II.
264 Recall that the sludge layer in Case IV has the same peak elevation as that in Case II but an
265 overall increased sludge volume (see Figure 2). As seen through Figures 4B and 4D, the
266 difference in the surface flow between Cases II and IV is that in the former, the jet is more
267 damped after passing over the sludge. This suggests that the short-circuiting in Case IV is
268 stronger than that in Case II, as will be confirmed further below. The greater short-circuiting in

269 Case IV compared to Case II may be ultimately attributed to conservation of mass as both cases
270 have the same flow rate with Case IV having the smaller water volume due to its greater amount
271 of sludge.

272 Figure 6A-L (upper 4 rows of panels) provides snapshots of tracer concentration on the x - y
273 (horizontal) plane at 0.69 m depth at 0.5, 2.0, and 4.0 days after initial tracer release for Cases I-
274 IV. Recall that the tracer is initially released with concentration $C = 1$ (g/L) at the inlet for a 17-
275 min period. At 0.5 day after initial release, the concentrated tracer patch is broken up by the
276 sludge for Cases II, III and IV. At 2.0 days after the initial release, the tracer in Case IV has
277 already reached the outlet, ahead of the tracer in Cases II and III. This is consistent with Figure 4
278 and the associated discussion earlier describing the greater short-circuiting at the surface in Case
279 IV compared to Case II.

280 The residence time distributions (RTDs) predicted by the simulations for Cases I-IV are
281 compared in Figure 7. A primary peak can be found in all four curves. The time at which the
282 primary peak occurs is mainly determined by the intensity of short-circuiting. For example,
283 occurrence of the RTD primary peak at earlier times corresponds to more intense short-circuiting.
284 In Figure 7, it can be seen that Case IV possesses the strongest short-circuiting (consistent with
285 earlier analysis), the short-circuiting in Cases I and II is almost identical and Case III has the
286 weakest short-circuiting.

287 The short-circuiting indices (S) for the four cases are calculated from Figure 7 and are listed in
288 Table 2. The short-circuiting index S is inversely proportional to the strength of short-circuiting
289 and thus proportional to hydraulic efficiency. As expected from previous analysis, S is smallest

290 for Case IV with a value of 0.07. Furthermore, the value of S ascends going in the following
291 order: Case IV (lowest), II, I, III (highest). The initial pond in 2006 with no sludge (Case I) has a
292 short-circuiting index of 0.089. Sludge accumulation by 2012 (Case II) causes the index to drop
293 to 0.075 indicating an increase in short circuiting. In particular, this drop is attributed to the
294 emergence of a strong jet over the sludge, as previously observed in terms of flow speed
295 contours in Figure 4. Between 2012 (Case II) and 2016 under Case III there is sludge build up in
296 such a way that the sludge baffling effect (described earlier) increases the short circuiting index
297 from 0.075 to 0.118 (i.e. reducing the strength of short-circuiting). However, between 2012
298 (Case II) and 2016 under Case IV, the sludge build up is such that the sludge baffling effect is
299 not enhanced as the index of Case IV is 0.07, the worst (lowest) of all 4 cases. The previous
300 observations about Cases II, III, and IV are consistent with their mean residence times of 21.89
301 days, 24.86 days and 20.36 days, respectively. Given that Cases III and IV have the same amount
302 of sludge, it can be concluded that sludge shape (geometry) plays an important role in
303 determining the hydraulic efficiency of the pond. Sludge deposited that reaches closer to the
304 surface of the water creates a greater baffling effect that increases the residence time and thus the
305 hydraulic efficiency of the pond (such as in Case III). In contrast, the same volume of sludge
306 spread more uniformly throughout the bottom of the pond reduces hydraulic efficiency (such as
307 in Case IV).

308 Although the sludge build up may seem beneficial in Case III, an increase in sludge reduces the
309 water volume treatment capacity of the pond. This is reflected through the higher relative
310 moment index for Case I (0.854) compared to Case III (0.606) in Table 2. Thus, there is a trade-

311 off between the gain in hydraulic efficiency and loss in water treatment capacity for Case III
312 compared to Case I when no sludge is present.

313 Overall, these findings have demonstrated that sludge distribution and volume have a significant
314 impact on wastewater hydraulic efficiency. Although treatment capacity is reduced with
315 accumulation of sludge, the latter may induce a baffling effect that can increase hydraulic
316 efficiency. As shown by Murphy (2012), sludge roughness has an impact on hydraulic
317 performance via dispersion. The present study demonstrates how the bulk sludge accumulation
318 can also have an impact via advection by re-directing the flow and potentially inducing a baffling
319 effect.

320

321 **Impact of water surface level change on hydraulic performance**

322 Results from flow and tracer transport simulations are based on the two approaches discussed
323 earlier for setting the surface water level (see Table 1). In the first approach the water surface
324 level for 2016 simulations (in Cases III and IV) was set equal to the water surface level of Case
325 II corresponding to the Lizima (2012) field measurements. In the second approach, the surface
326 water levels for 2016 simulations (in Cases IIIA and IVA) were set to maintain the same water
327 volume measured in the field by Lizima (2012). Thus Cases III and IIIA have the same sludge
328 distribution, but different water surface levels. The same applies for Cases IV and IVA. For each
329 of these cases, three snapshots of the tracer concentration at the surface of the pond $t=0.5$ day,
330 $t=2$ days and $t=4$ days (after release of the tracer) are plotted in Figure 6M-X (lower four rows of
331 panels).

332
333 Comparing Case III with Case IIIA or IV with IVA, major differences in flow patterns at the
334 surface and ultimately in residence times are noted due to changes in water surface elevation. For
335 example, at time $t=0.5$ day for Case IIIA (Figure 6P) the tracer route is partially obstructed by
336 the sludge. In this simulation, although the sludge still acts like a baffle as described earlier, the
337 increase in water surface level (compared to Case III in Figure 6M-O) allows part of the tracer to
338 flow over the top of the sludge following a more direct route to the outlet. This more direct route
339 results in greater short-circuiting. In Case III (Figure 6M-O), the baffling effect of the sludge is
340 greater compared to Case IIIA (Fig. 6P-R) as a greater amount of the tracer is diverted by the
341 sludge and redirected towards the sidewalls of the pond in the former simulation. Similar
342 conclusions can be made comparing Cases IV and IVA in Figure 6S-X. At time $t=2$ days after
343 the release of the tracer, Cases IIIA and IVA (panels 6Q and 6W) show that a majority of the
344 tracer has exited the pond compared to Cases III and IV (panels 6N and 6T), consistent with the
345 greater short-circuiting induced by the higher water surface elevation in IIIA and IVA.

346
347 Short-circuiting indexes are listed in Table 3. In Case IIIA, the short-circuiting index is less than
348 in Case III (0.066 compared with 0.118), thus stronger short-circuiting occurs in the former
349 simulation, as previously concluded. Analogous results are observed when comparing Cases IV
350 and IVA with the short-circuiting indexes of 0.07 for Case IV and 0.05 for Case IVA (higher
351 water surface elevation).

352
353 Overall, it is seen that an increase in water surface elevation can diminish the potential baffling
354 effect induced by the sludge by opening up a path for the water to flow over the sludge. This is

355 consistent with results from the previous sub-section showing that sludge accumulation reaching
356 closer to the surface leads to a greater baffling effect.

357

358 **CONCLUSIONS**

359 The present CFD study, based on physically measured and future predictions of sludge
360 accumulation, demonstrates that an increase in sludge volume (depending on the sludge
361 distribution or geometry) may improve the hydraulic performance of a WSP by inducing a
362 baffling effect. For example, sludge accumulation reaching closer to the surface of the water was
363 seen to be beneficial by preventing short-circuiting over the sludge and thus providing a greater
364 baffling effect. This is an important benefit because many of these systems are not constructed
365 with influent baffles. However, a tradeoff of this benefit is that sludge accumulation reduces the
366 treatment capacity of the WSP. Furthermore, it was found that an increase in water surface
367 elevation reduces the baffling effect of the sludge by allowing significant flow over the sludge
368 thereby promoting short-circuiting, resulting in decrease in hydraulic efficiency. These results
369 demonstrate the importance of performance monitoring and the duration of such monitoring
370 given the long-term dynamic impact of sludge accumulation coupled with water surface
371 elevation on WSP hydraulic performance. Unfortunately rural water and sanitation systems in
372 the developing world have proven easier to construct than to maintain (Schweitzer & Mihelcic,
373 2012).

374

375 The important interplay between sludge accumulation and water surface level determining
376 hydraulic performance, highlighted in this study, suggests that the creation of a future CFD

377 model capable of dynamically calculating the water surface level given a sludge
378 distribution/amount and flow rate would be of great benefit. Dispersion caused by sludge surface
379 roughness had been previously found to also impact hydraulic performance (Murphy, 2012);
380 because sludge roughness is not considered in the present study, further study should be
381 conducted to investigate the combined effect and relationship between sludge accumulation and
382 distribution, sludge roughness, and water surface level.

383
384 This study found that the distribution of sludge in a WSP is critical for determining its hydraulic
385 performance. A better understanding of sludge accumulation could be obtained using a more
386 advanced CFD model, such as a liquid-solid two-phase flow model, which would dynamically
387 couple and compute sludge distribution and water surface level. An alternative, more practical
388 approach would be the use of single-phase CFD as in this study aided by physical measurements
389 of sludge distribution in typical (standard) pond configurations. It is recommended that operators
390 measure sludge accumulation and pond water surface level over long term in standard,
391 commonly used pond configurations. Based on the data compiled, CFD may be utilized to
392 evaluate the long-term hydraulic performance of these WSPs. This information could be
393 tabulated and provided to managers to better determine the current and future hydraulic
394 performance of existing and future WSPs and ultimately establish a desludging schedule that
395 could optimize pond usage and performance.

396
397 Finally, the results obtained here demonstrate the importance of baffling, thereby highlighting
398 some of the benefits that could be gained by designing and building WSPs with physical baffles.

399

400

401 **Acknowledgements**

402 This material is based upon work supported by the National Science Foundation under Grant No.
403 1243510. Cornejo was supported by the NSF FGLSAMP Bridge to the Doctorate Award,
404 McKnight Doctoral Fellowship, and Sloan Minority PhD program.

405

406 **REFERENCES**

- 407 Alvarado, A., Sanchez, E., Durazno, G., Vesvikar, M., & Nopens, I., 2012. CFD analysis of
408 sludge accumulation and hydraulic performance of a waste stabilization pond. *Water*
409 *Science and Technology*, 66:11:2370-2377.
- 410 Alvaro Mercado, Olver Coronado, Mercedes Iriarte, 2013. Evaluación del funcionamiento de la
411 planta de tratamiento de aguas residuales de Punata, Cochabamba, Bolivia. Importancia de
412 la Operación y mantenimiento, XV Congreso Bolivariano de Ingeniería Sanitaria y
413 Ambiental.
- 414 Brauer, F., & Castillo-Chávez, C., 2011. Mathematical models in population biology and
415 epidemiology. Springer, New York, NY, USA.
- 416 Canale, R. P., Auer, M. T., Owens, E. M., Heidtke, T. M., & Effler, S. W., 1993. Modeling fecal
417 coliform bacteria—II. Model development and application. *Water Research*, 27:4:703-714.
- 418 Cornejo, P. K., Zhang, Q., & Mihelcic, J. R., 2013. Quantifying benefits of resource recovery
419 from sanitation provision in a developing world setting, *Journal of Environmental*
420 *Management*, 131:7-15.

- 421 Ferrara, R. A., & Harleman, D. R., 1981. Hydraulic modeling for waste stabilization ponds.
422 *Journal of the Environmental Engineering*, 107:4:817-830.
- 423 Fuchs, V.J., & Mihelcic, J.R., 2011. Analyzing appropriateness in sanitation projects in the Alto
424 Beni region of Bolivia. *Waterlines*, 30:122-134.
- 425 Goncalves, R. F., Taveira, E. J. A., Cassini, S. T. A., & de Oliveira, F. F., 2002. Recycled sludge
426 thickening and digestion pond from physicochemical upgrading process of facultative
427 pond effluent. International IWA Specialist Group Conference on Waste Stabilization in
428 Ponds, Auckland, New Zealand.
- 429 Holland, JF, Martin, JF, Granata, T, Bouchard, V, Quigley, M & Brown, L., 2004. Effects of
430 wetland depth and flow rate on residence time distribution characteristics, *Ecological*
431 *Engineering*, 23:3:189-203.
- 432 Karteris, A., Papadopoulos, A., & Balafoutas, G., 2005. Modeling the temperature pattern of a
433 covered anaerobic pond with computational fluid dynamics. *Water Air Soil Pollution*,
434 162:107-125.
- 435 Konate, Y., Maiga, A., Wethe, J., Casellas, C. & Picot, B., 2011. Sludge accumulation in
436 stabilization ponds in the Soudano-Sahelian climate of Burkina Faso. Journées
437 scientifiques du 2IE, Ouagadougou, Burkina Faso.
- 438 Launder, B. E., 1978. Heat and mass transport. Turbulence, Chap. 6, P. Bradshaw, ed., Springer,
439 Berlin.
- 440 Lizima, L., 2012. Hydraulic evaluation of a community managed wastewater stabilization pond
441 system in Bolivia. Master's Thesis, University of South Florida.

- 442 Lloyd, B., Vorkas, C., & Guganesharajah, R., 2003. Reducing hydraulic short-circuiting in
443 maturation ponds to maximize pathogen removal using channels and wind breaks. *Water*
444 *Science & Technology*, 48:2:153-162.
- 445 Mara, D. D., 2004. Domestic wastewater treatment in developing countries, Earthscan
446 Publications, London.
- 447 Mayo, A. W., 1995. Modeling coliform mortality in waste stabilization ponds. *Journal of*
448 *Environmental Engineering*, 121:2:140-152.
- 449 Min, JH & Wise, WR, 2009. Simulating short-circuiting flow in a constructed wetland: the
450 implications of bathymetry and vegetation effects, *Hydrological Processes*, 23:830-841.
- 451 Muga, H.E. & Mihelcic, J.R., 2008. Sustainability of Wastewater Treatment Technologies,
452 *Journal of Environmental Management*, 88: 437-447.
- 453 Murphy, C, 2012. Quantifying the Impact of Sludge Accumulation on the Hydraulic
454 Performance of Waste Stabilization Ponds. Bachelor's thesis, University of Western
455 Australia.
- 456 Nelson, K., Cisneros, B., Tchobanoglous, G. & Darby, J. 2004. Sludge accumulation,
457 characteristics, and pathogen inactivation in four primary waste stabilization ponds in
458 central Mexico, *Water Research*, 38:1:111-127.
- 459 Oakley, S. M., 2005. Lagunas de Estabilización en Honduras: Manual de Diseño, Construcción,
460 Operación y Mantenimiento, Monitoreo y Sostenibilidad. United States Agency for
461 International Development-Honduras (USAID-Honduras), Red Regional de Agua y
462 Saneamiento para Centro América (RRAS-CA), Fondo Hondureño de Inversión Social
463 (FHIS), Tegucigalpa, Honduras.

- 464 Oakley, S. M., Mendoca, L. C., & Mendoca, S. R., 2012. Sludge removal from primary
465 wastewater stabilization ponds with excessive accumulation: a sustainable method for
466 developing regions. *Journal of Water, Sanitation, and Hygiene for Development*, 2:2:68-
467 78.
- 468 OpenFOAM User Guide version 1.7.1, 2010. OpenCFD Ltd. <[http://www.openfoam.com](http://www.openfoam.com/docs/user/)
469 /docs/user/> (accessed Jul. 10, 2014)
- 470 Papadopoulos, A., Papadopoulos, F., Parisopoulos, G. & Karteris, A., 2003. Sludge
471 accumulation pattern in an anaerobic pond under Mediterranean climatic conditions. *Water*
472 *Research*, 37:3:634-644.
- 473 Peña, M. R., Mara, D. D., & Sanchez, A., 2000. Dispersion studies in anaerobic
474 ponds: implications for design and operation. *Water Science and Technology*, 42, 273-282.
- 475 Perssoen, J. 2000. The hydraulic performance of ponds of various layouts. *Urban Water*,
476 2:3:243-250.
- 477 Peterson, E. L., Harris, J. A., & Wadhwa, L. C., 2000. CFD modeling pond dynamic processes.
478 *Aquacultural Engineering*, 23:61-93.
- 479 Polprasert, C., & Bhattarai, K. K. 1985. Dispersion model for waste stabilization ponds. *Journal*
480 *of Environmental Engineering*, 111:1:45-59.
- 481 Schweitzer, R.W., Mihelcic, J.R., 2012. Sustainability Analysis of Community Managed Water
482 Systems in the Developing World, *Journal of Water, Sanitation and Hygiene for*
483 *Development*, 2:1:20-30.
- 484 Shilton, A., 2000. Potential application of computational fluid dynamics to pond design. *Water*
485 *Science and Technology*, 42:327-334.

- 486 Shilton, A., Kreegher, S., & Grigg, N., 2008. Comparison of computation fluid dynamics
487 simulation against tracer data from a scale model and full-sized waste stabilization pond.
488 *Journal of Environmental Engineering*, 134:845-850.
- 489 Sweeney, D. G., Nixon, J. B., Cromar, N. J., & Fallowfield, H. J., 2005. Profiling and modelling
490 of thermal changes in a large waste stabilization pond. *Water Science and Technology*,
491 51:163-172.
- 492 Symonds, E.M., Verbyla, M.E., Kafle, R.C., Lukasik, J.O., Breitbart, M., Mihelcic, J.R., 2014. A
493 case study of enteric virus removal and insights into the associated risk of water reuse for
494 two wastewater treatment pond systems in Bolivia, *Water Research*, 65:257-270.
- 495 Teixeira, E.C., & Siqueira, R.N., 2008. Performance Assessment of Hydraulic Efficiency
496 Indexes. *Journal of Environmental Engineering*, 134:10:851-859.
- 497 Vega, G. P., Pena, M. R., Ramirez, C., & Mara, D. D., 2003. Application of CFD modelling to
498 study the hydrodynamics of various anaerobic pond configurations. *Water Science and*
499 *Technology*, 48:163-171.
- 500 Verbyla, M. E., Oakley, S. M., & Mihelcic, J. R., 2013a. Wastewater infrastructure for small
501 cities in an urbanizing world: Integrating the protection of human health and the
502 environment with resource recovery and food security. *Environmental Science &*
503 *Technology*, 47:8:3598–3605.
- 504 Verbyla, M. E., Oakley, S. M., Lizima, L. A., Zhang, J., Iriarte, M., Tejada-Martinez, A. E., &
505 Mihelcic, J. R., 2013b. Taenia eggs in waste stabilization pond systems with poor
506 hydraulics: Concern for human cysticercosis? *Water Science and Technology*. 68:12:2698-
507 2703.

- 508 Verbyla, M.E., Mihelcic, J.R., 2015. A review of virus removal in wastewater treatment pond
509 systems, *Water Research*, 71:107-124.
- 510 Wahl, MD, Brown, LC, Soboyejo, AO, Martin, J & Dong, B, 2010. Quantifying the hydraulic
511 performance of treatment wetlands using the moment index, *Ecological Engineering*,
512 36:1691-1699.
- 513 Wilcox, D. C., 1994. Turbulence Modeling for CFD. DCW Industries, Inc., La Cañada Flintridge,
514 California.
- 515 Wood, M. G., Greenfield, P. F., Howes, T., Johns, M. R., & Keller, J., 1995. Computational fluid
516 dynamic modeling of waste-water ponds to improve design. *Water Science and*
517 *Technology*, 31:111-118.
- 518 Wood, M. G., Howes, T., Keller, J., & Johns, M. R., 1998. Two dimensional computational fluid
519 dynamic models for waste stabilisation ponds. *Water Research*, 32:958-963.
- 520 Zhang, J., Tejada-Martínez, A. E., & Zhang, Q., 2013a. RANS simulation of the flow and tracer
521 transport in a multi-chambered ozone contactor. *Journal of Environmental Engineering*,
522 139:3:450-454.
- 523 Zhang, J., Tejada-Martínez, A. E., & Zhang, Q., 2013b. Hydraulic efficiency in RANS of the
524 flow in multi-chambered ozone contactors, *Journal of Hydraulic Engineering*,
525 139:11:1150-1157.
- 526 Zhang, J., Tejada-Martinez, A. E., Zhang, Q., & Lei, H., 2014a. Evaluating Hydraulic and
527 Disinfection Efficiencies of a Full-Scale Ozone Contactor using a RANS-based Modeling
528 Framework, *Water Research*, 52:155-167.

529 Zhang, J., Tejada-Martínez, A. E., & Zhang, Q., 2014b. Evaluation of LES and RANS for
530 Determining Hydraulic Performance of Water Disinfection Systems, *Journal of Fluid*
531 *Engineering*, 136(12), 121102.
532

Table 1: Water volumes, sludge volumes and water surface elevations for Cases I-IV, IIIA and IVA.

Cases	Sludge Volume (m ³)	Water Volume (m ³)	Water Surface Elevation (m)
Case I	0	1979	1.8
Case II	154	1815	1.8
Case III	326	1643	1.8
Case IV	326	1643	1.8
Case IIIA	326	1815	1.944
Case IVA	326	1815	1.944

Table 2: Comparison of treatment efficiency indices and residence times for Cases I-IV.

Cases	S	Theoretical residence time τ	CFD-predicted mean residence time $\bar{\tau}$	Moment Index	Relative Moment Index
Case I	0.089	29.98	22.93	0.854	0.854
Case II	0.075	27.65	21.89	0.781	0.720
Case III	0.118	25.04	24.86	0.7998	0.606
Case IV	0.07	25.04	20.36	0.7994	0.606

Table 3: Comparison of short-circuiting indices in Cases III, IV, IIIA and IVA

Cases	Short Circuiting Index	Water Surface Level (m)
Case III	0.066	1.8
Case IIIA	0.118	1.95
Case IV	0.05	1.8
Case IVA	0.07	1.95

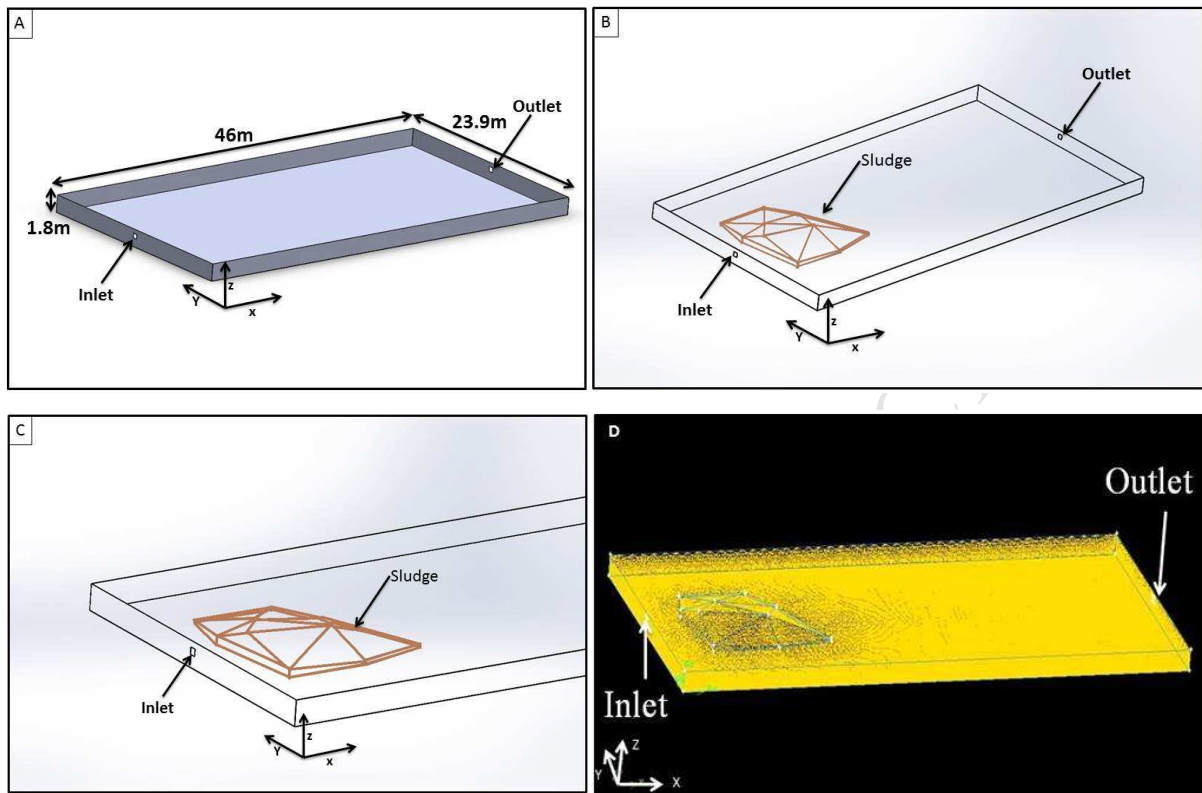


Figure 1: (A) Pond in 2006 with no sludge. Pond length is 46 m, width is 23.9 m and height is 1.8m; the inlet and outlet cross-sectional areas are 0.25 m^2 each. (B) Computational domain based on sludge profile physically measured in 2012 (Case II). (C) Close up view of inlet and sludge. (D) Corresponding computational mesh consisting of tetrahedral elements.

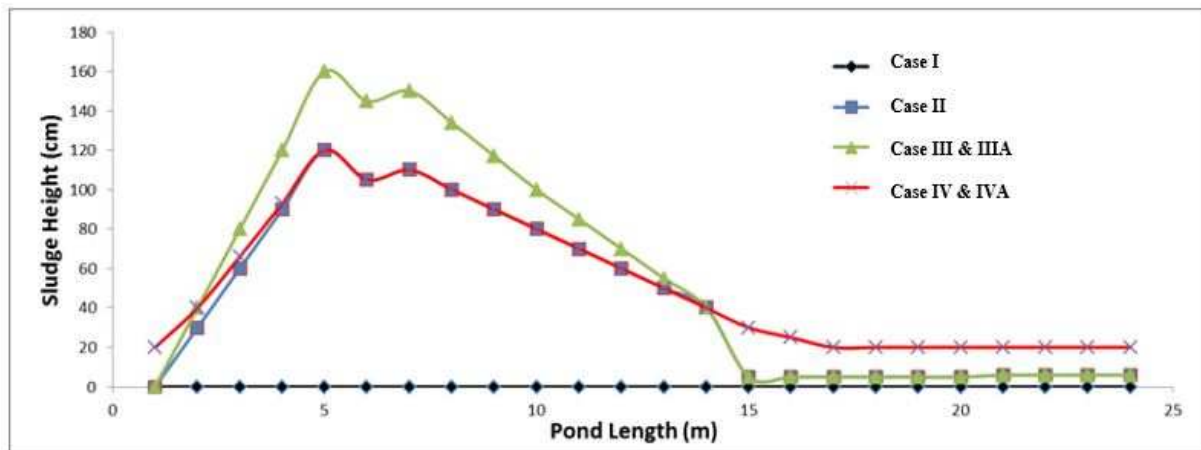


Figure 2: Comparison of the sludge profiles on x - z plane at mid-span of the pond for cases I-IV.

Case I corresponds to the WSP with no sludge (2006). Case II corresponds to the field measurements of Lizima, 2012 and Case III & IV correspond to projected sludge accumulations in 2016.

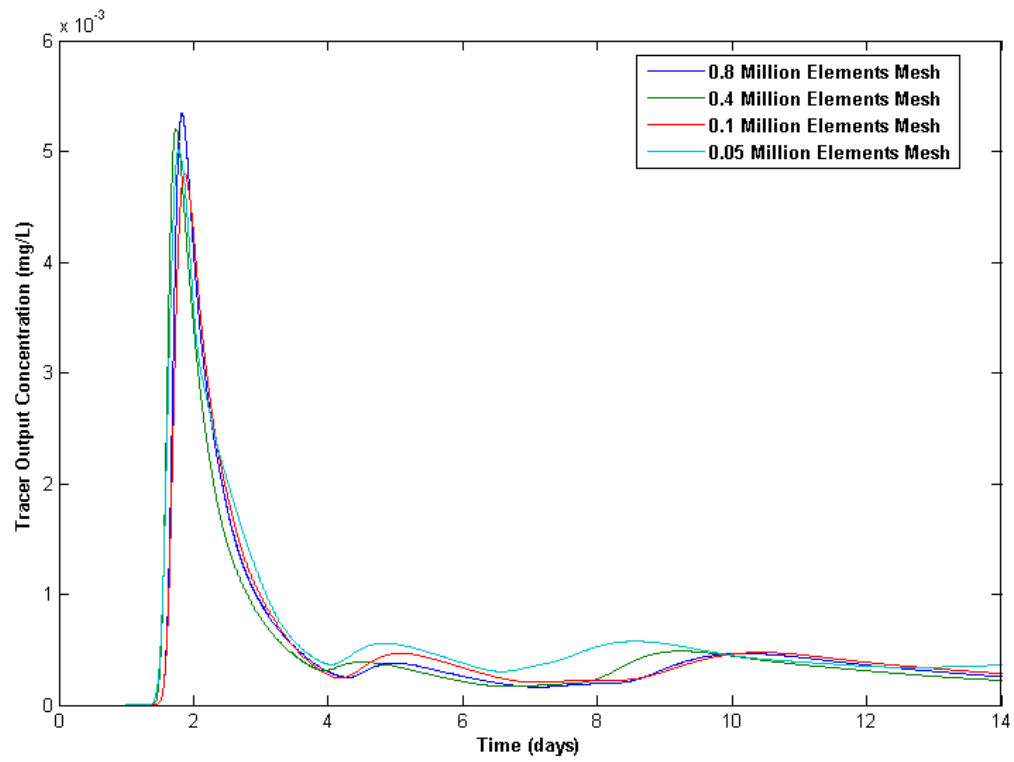


Figure 3: Grid convergence study for Case II.

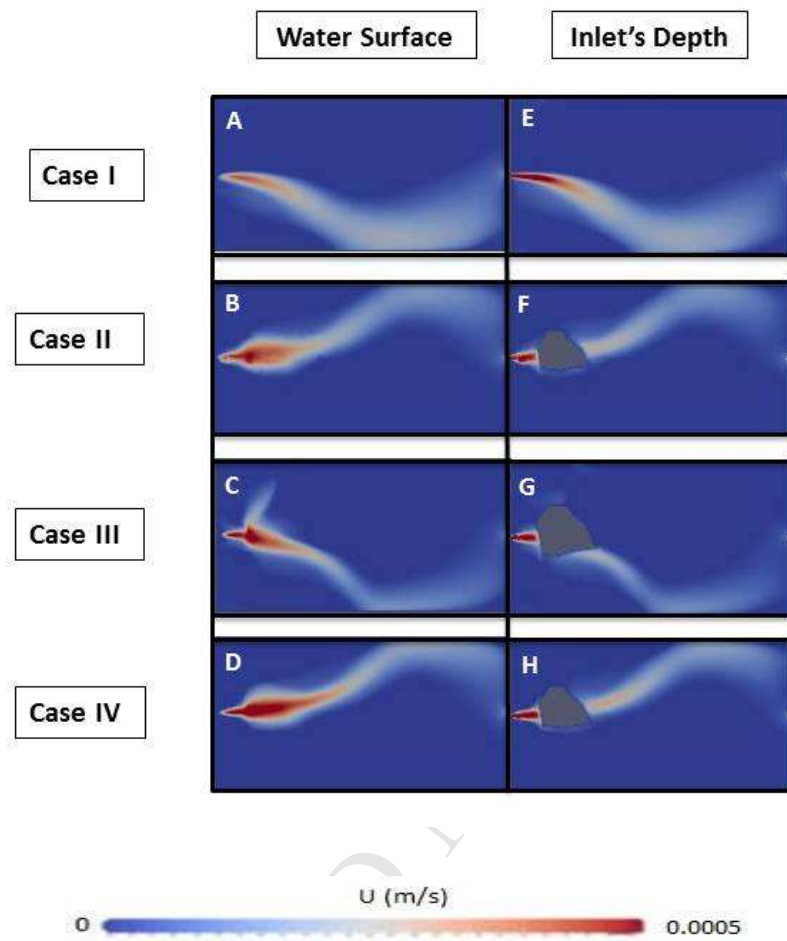


Figure 4: Water flow speed contours for Cases I-IV on x - y (horizontal) planes at depth = 0 m (corresponding to the water surface) and depth = 0.69 m below the water surface (at the depth of the inlet). The sludge accumulation is color-coded gray.

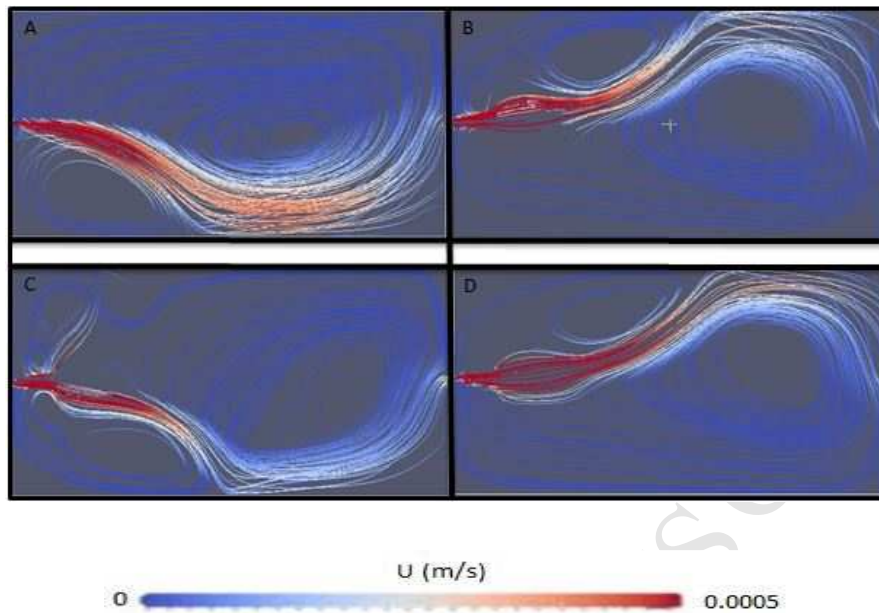


Figure 5: Streamlines superimposed with flow speed contours for different sludge accumulation scenarios viewed from above the pond (top view) for Case I (panel A), Case II (B), Case III (C) and Case IV (D).

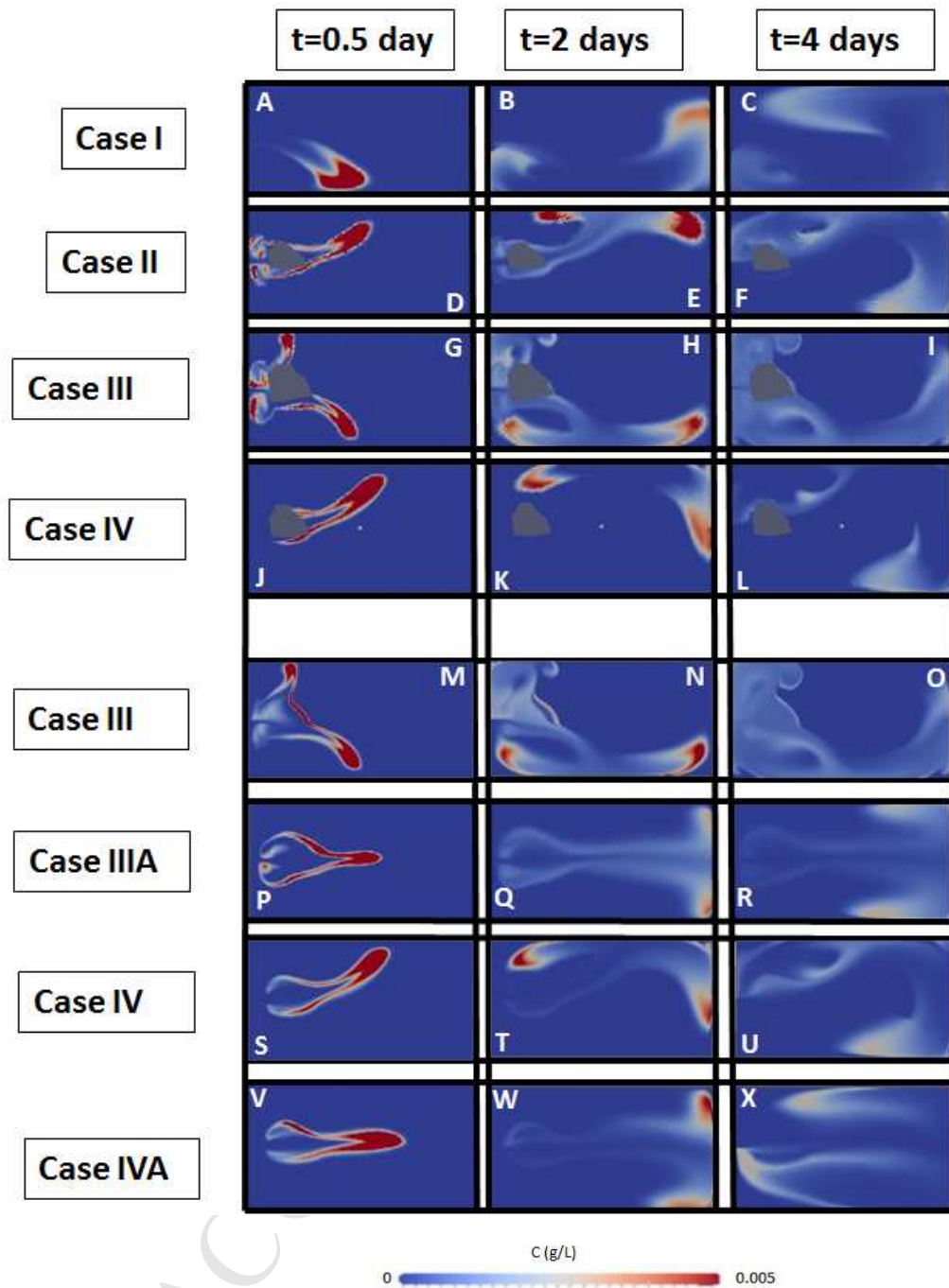


Figure 6: Snapshots of normalized tracer transport on the x-y (horizontal) at different times ($t = 0.5, 2.0, \text{ and } 4.0$ days). Panels A-L are at the depth 0.69m (inlet location) the sludge accumulation is color-coded gray; and M-X are at the water surface.

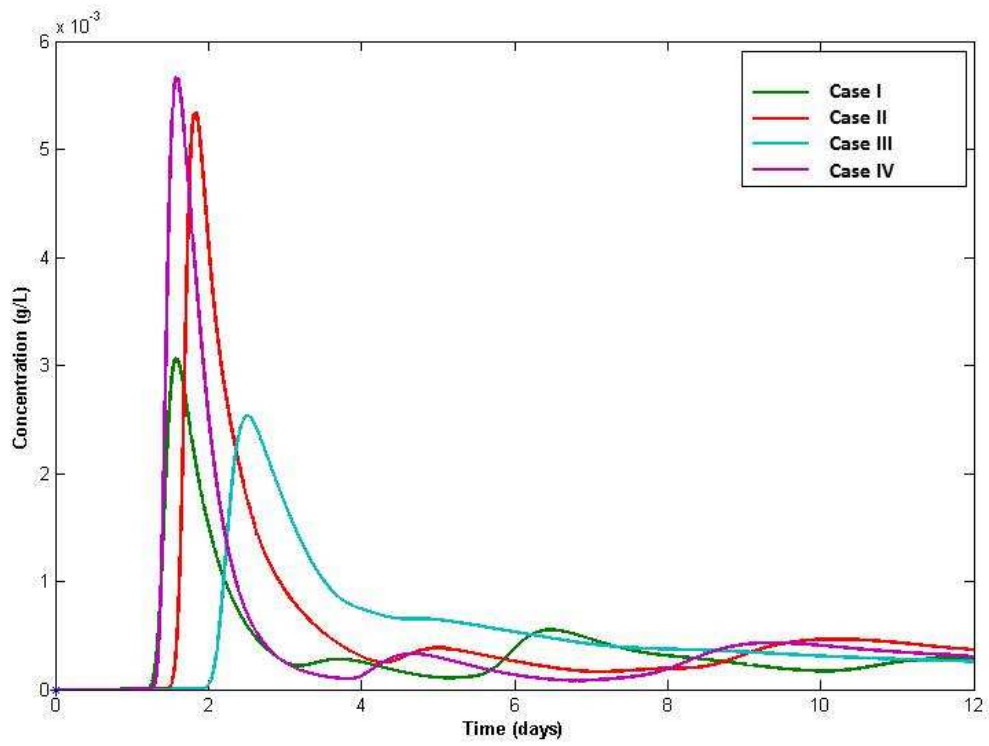


Figure 7: Comparison of residence time distribution (RTD) curves for Cases I-IV.

Impact of Sludge Layer Geometry on the Hydraulic Performance of a Waste Stabilization Pond

Highlights:

- CFD analysis of a waste stabilization pond (WSP) with bottom sludge is presented.
- Sludge induces a baffling effect and thus may improve hydraulic efficiency.
- Increase in water surface elevation reduces baffling effect via short-circuiting.
- Various metrics are calculated in order to quantify the baffling effect.
- CFD can be an invaluable tool for WSP managers to track pond hydraulic performance.